

MESOSIDERITES ON VESTA: A HYPERSPECTRAL VIS-NIR INVESTIGATION E. Palomba (1), A. Longobardo (1), M.C. De Sanctis (1), D. W. Mittlefehldt (2), E. Ammannito (1), F. Capaccioni (1), M.T. Capria (1), A. Frigeri (1), F. Tosi (1), F. Zambon (1), C.T. Russell (3), C.A. Raymond (4)

(1) INAF-IAPS, Rome, Italy, ernesto.palomba@iaps.inaf.it, (2) NASA/Johnson Space Center, Houston, TX, USA (3) UCLA, Los Angeles, USA, (4) Cal. Inst. Tech JPL, Pasadena, USA

Introduction: The discussion about the mesosiderite origin is an open issue since several years. Mesosiderites are mixtures of silicate mineral fragments or clasts, embedded in a FeNi metal matrix. Silicates are very similar in mineralogy and texture to howardites [1]. This led some scientists to conclude that mesosiderites could come from the same parent parent asteroid of the howardite, eucrite and diogenite (HED) meteorites [2, 3]. Other studies found a number of differences between HEDs and mesosiderite silicates that could be explained only by separate parent asteroids [4].

Recently, high precision oxygen isotope measurements of mesosiderites silicate fraction were found to be isotopically identical to the HEDs, requiring common parent body, i.e. 4 Vesta [5]. Another important element in favor of a common origin was given by the identification of a centimeter-sized mesosiderite clast in a howardite (Dar al Gani 779): a metal-rich inclusion with fragments of olivine, anorthite, and orthopyroxene plus minor amounts of chromite, tridymite, and troilite [6]. The Dawn mission with its instruments, the Infrared Mapping Spectrometer (VIR) [7], the Framing Camera [8] and the Gamma-Ray and Neutron Detector (GRaND) [9] confirmed that Vesta has a composition fully compatible with HED meteorites [10]. We investigate here the possibility to discern mesosiderite rich locations on the surface of Vesta by means of hyperspectral IR images.

Mesosiderite spectral behavior: Mesosiderite Vis-Nir spectra have a spectral behavior similar to a typical pyroxene and are dependent on the abundance of the metallic phases, which tend to decrease the overall I/F and in some cases to slightly change slopes. Therefore, discerning mesosiderite signatures from the typical Eucritic, Howarditic, Diogenitic behavior we observe on Vesta can be a very tricky task.

Samples: We tried to define one or more spectral indicator, which could allow to discern mesosiderite from other Vestan main mineralogical components (i.e. pyroxenes). Therefore, a detailed selection and analysis has been performed on RELAB spectra of different kinds of HEDs and mesosiderites. Since for the mesosiderite spectra that are available size are not characterized (Estherville, Vaca Muerta, Pinnaroo, Lamont), it is important to study the effect of grain size on the considered spectral indicators. For this reason, spectra corresponding to HED (Juvinas, millbillillie, ALH

A76005, Y-74450, EET A79002) at different grain sizes (0-25, 25-45, 45-75, 75-125 and 125-250 μm) were selected: these spectra are described in [11].

Dark chondrites: Dark ordinary chondrites (OC) are an instructive case: they contain abundant metal phases and, differently from typical OC, their IR reflectance is similar to mesosiderites, for this reason, spectra of ordinary chondrites (Tsarev, Farmington and Castalia) have been selected and tested. Different grain sized samples of Tsarev (0-63, 63-125, 125-250 and 250-500 μm of dark lithology and 0-25, 25-45, 45-63, 63-125 and 125-250 μm of light lithology) and Farmington (20-250 μm and slab) have been considered.

Carbonaceous chondrites: Three carbonaceous chondrites (Cold Bokkevelt-CM, Orgueil-CI and Grosnaja-CV) at different grain sizes (0-75, 75-150 and 150-500 μm for Cold Bokkevelt and Grosnaja and 0-40, 40-100 and 100-200 μm for Orgueil) have been considered, too.

Definition of mesosiderite spectral indicators:

I/F @ 0.68 μm

The main difference between the two materials, is the mesosiderite lower reflectance, induced by the low reflectance and neutral behaviors of the metal phases. However, the I/F alone cannot be used as an indicator to identify mesosiderites, since many dark materials deposits exist on Vesta that seems to have originated mainly from carbonaceous chondrites impacted on Vesta [12].

BAR

Since the Band Area Ratio (BAR) value depends on how the spectral intervals for the computation are chosen, we use here the BAR as defined in [13].

OLVIndex

This spectral indicator is defined in [14] and is used for detection of olivine. However, we found is very sensible to the presence of metals, thus we tried to test it as a mesosiderite indicator.

Results: To better separate mesosiderites from dark chondrites and from HEDs we built scatterplots by coupling together the different spectral indicators. In the BAR vs OLVIndex, HEDs and mesosiderites are placed closely and is nearly impossible to separate the two populations. In the I/F vs BAR (Fig. 1) the three populations appear separated. However, by decreasing grain size, I/F increases and BAR decreases. This

means that fine grained mesosiderites could shift towards the HEDs cloud (as indicated by the brown arrow), making a clear distinction very tricky. On the contrary, mesosiderites and OCs remain well separated. In the I/F vs OLVIndex mesosiderites are partially grouped with chondrites (dark OCs and carbonaceous chondrites, but are separated from HEDs (Fig. 2). In this case, decreasing grain size does not generate confusion: both I/F and OLVIndex increase, and the fine grained mesosiderites would move in a region (red arrows) away from HED.

Furthermore, a combined use of the two scatterplots can help to discern mesosiderites from HEDs (I/F vs OLVIndex) and from OCs (I/F vs BAR).

We preliminarily applied these scatterplots to the VIR observation of Vesta (not photometrically corrected). In order to reduce possible influences of the observing conditions we had to select only the observations in a narrow interval of emission and incidence angles $40^\circ < i, e < 50^\circ$. Results on this very limited dataset don't show evidence of locations that have behaviors clearly different from the average Vestan regions. Our next steps include: a photometric correction (by using the Hapke relation) and extension of the analysis on the entire VIR dataset and laboratory measurements of new mesosiderite samples, possibly for different grain size intervals.

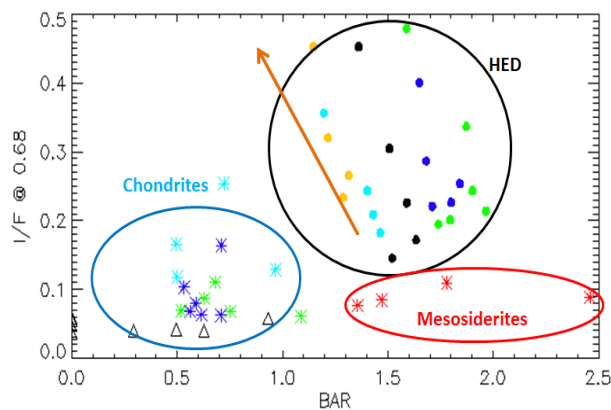


Figure 1. Scatterplot of I/F at 0.68 microns as function of BAR. Dots indicates different grain sized HEDs (each color correspond to a HED), green and blue asterisks correspond to Tsarev (dark and light lithologies respectively), cyan asterisks to dark chondrites, whereas triangles and red asterisks indicate carbonaceous chondrites and bulk mesosiderites, respectively. The brown arrow indicates the possible direction of displacement of mesosiderites in the scatterplot at decreasing grain size.

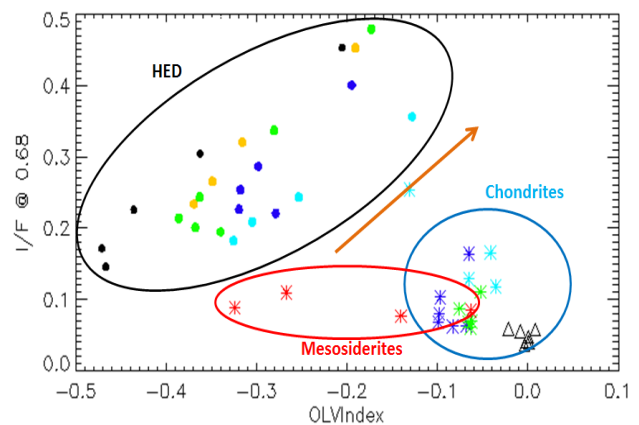


Figure 2. Scatterplot of I/F at 0.68 microns as function of OLVIndex. Dots indicates different grain sized HEDs (each color correspond to a HED), green and blue asterisks correspond to Tsarev (dark and light lithologies respectively), cyan asterisks to dark chondrites, whereas triangles and red asterisks indicate carbonaceous chondrites and bulk mesosiderites, respectively. The brown arrow indicates the possible direction of displacement of mesosiderites in the scatterplot at decreasing grain size.

References: [1] Mittlefehldt, D. W. et al. (1998) *Rev. in Mineral*, 36, chapter 4 [2] Duke, M. B. and Silver, L. T. (1967) *GCA* 31, 1637–1665 [3] Powell, B. N. (1971) *GCA* 35, 5–34 [4] Mittlefehldt, D. W. (1990) *GCA* 54, 1165–1173 [5] Greenwood, R. C. et al. (2006) *Science*, 313, 1763–1765 [6] Rosing, M. T. and Haack, H. (2004) *LPSC XXXV*, Abstract #1487 [7] De Sanctis, M.C. et al. (2011) *SSR* 163 [8] Sierks, H. et al. (2011) *SSR* doi: 10.1007/s11214-011-9745-4 [9] Prettyman, T.H. et al. (2011) *SSR*, doi:10.1007/s11214-011-9862-0 [10] De Sanctis, M.C. et al., (2012) *Science* 336, 697–700 [11] Duffard, R. et al. (2005), *MAPS* 40, 3, 445–459 (Appendix III) [12] McCord, T.B. et al. (2012), *Nature*, 491, 83–86 [13] Cloutis, E.A. et al. (1986) *JGR* 91, 11641–11653 [14] Carrozzo, F.G. et al. (2012) *JGR*, 117, E00J17